



Freezing Efficiency and Quality Attributes as Affected by Voids in Plant Tissues During Ultrasound-Assisted Immersion Freezing

Zhiwei Zhu^{1,2,3} · Zhubing Chen^{1,2,3} · Qianyun Zhou^{1,2,3} · Da-Wen Sun^{1,2,3,4} · Haiyang Chen⁵ · Yongjun Zhao⁶ · Wenqing Zhou⁷ · Xianguang Li⁸ · Hongzhun Pan⁸

Received: 4 February 2018 / Accepted: 5 April 2018 / Published online: 13 June 2018
© Springer Science+Business Media, LLC, part of Springer Nature 2018

Abstract

Voids, filled with air, in plant tissues, can attenuate ultrasound, resulting in weakening the effectiveness of ultrasound during immersion freezing. The effect of voids on ultrasound-assisted immersion freezing (UF) in selected plant tissues, apple, radish, and potato was investigated in the present study. The freezing time and quality attributes of firmness, drip loss, total calcium content, and total phenolic content were investigated in apple, radish, and potato samples treated by normal immersion freezing (IF) and UF. The results showed that the more the percentage voids in the plant tissues, the lower the effectiveness of the ultrasound treatment. The total freezing time reduction (%) due to UF was a power function of the volume of voids (%): $y = 0.018x^{-1.057}$ ($R^2 = 0.994$). Ultrasound at 0.62 W/cm^2 (28 kHz) resulted in the best firmness and lowest drip loss in potato, while no significant ($p > 0.05$) differences in quality attributes were observed between IF and UF in apple samples. These findings indicated that UF was more effective in freezing fruit or vegetables with a highly dense structure.

Keywords Ultrasound attenuation · Freezing time · Microstructure · Drip loss · Firmness · Plant tissue

Introduction

Like drying (Sun and Woods 1994a, b and c; Sun and Woods 1993; Sun 1999; Yang et al. 2017; Pu and Sun 2016; Qu et al. 2017a; Ma et al. 2017; Pu and Sun 2017) and cooling (Wang and Sun 2001; McDonald et al. 2001; McDonald and Sun 2001; Hu and Sun 2000; Sun and Eames 1996; Desmond et al. 2000), freezing is an effective method for long-term preservation of perishable food products (Kiani et al. 2012; Ma et al. 2015; Xie et al. 2015; Cheng et al. 2016; Pu et al. 2015; Cheng et al. 2017; Xie et al. 2016; Qu et al. 2017b; Cheng et al. 2018).

However, traditional freezing technologies, including air blast freezing, plate contact freezing, fluidized-bed freezing, immersion freezing, and cryogenic freezing (Islam et al. 2017), are based on temperature difference as the driving force to achieve the heat transfer between food products and the freezing medium. Generally, the thermal conductivity of foods is approximately $0.5\text{--}1.5 \text{ W m}^{-1} \text{ K}^{-1}$ (Sun and Li 2003), which limits the freezing rate. Owing to a high water content in fresh fruits and vegetables, normally large ice crystals are formed in food products during slow freezing processes, and these large ice crystals are mainly located in the extracellular region (Zheng

✉ Da-Wen Sun
dawen.sun@ucd.ie; <https://www.ucd.ie/refrig>; <https://www.ucd.ie/sun>

¹ School of Food Science and Engineering, South China University of Technology, Guangzhou 510641, China

² Academy of Contemporary Food Engineering, South China University of Technology, Guangzhou Higher Education Mega Center, Guangzhou 510006, China

³ Engineering and Technological Research Centre of Guangdong Province on Intelligent Sensing and Process Control of Cold Chain Foods, Guangzhou Higher Education Mega Centre, Guangzhou 510006, China

⁴ Food Refrigeration and Computerized Food Technology (FRCFT), Agriculture and Food Science Centre, University College Dublin, National University of Ireland, Belfield, Dublin 4, Ireland

⁵ Shenzhen Dejieli Refrigeration Technology Co., Ltd., Gongming Street, Guangming District, Shenzhen 518106, China

⁶ Chengdu Rodbol Machinery Equipment Co., Ltd., Deyuan Town, Pidu District, Chengdu 611730, China

⁷ Foshan Suk Precision Machinery Co., Ltd., Luocun Town, Nanhai District, Foshan 528226, China

⁸ Guangzhou Yuelian Fisheries Refrigeration Engineering Co., Ltd., Daban Industrial Zone, Panyu District, Guangzhou 511490, China

and Sun 2006; Góral and Kluza 2009), which could rupture the cellular structure irreversibly, causing poor sensory properties and the loss of nutrients (Alvarez et al. 2005; Koushki et al. 2013). It is generally accepted that rapid freezing generates smaller ice crystals, resulting in less mechanical damage to the cell structure, while slow freezing forms large ice crystals, causing serious mechanical damage to materials (Sanz et al. 1999; Li and Sun 2002). However, some researches indicated that calcium in plants helps to maintain the structure and integrity of cell wall, thus reducing the damage caused by ice crystals (Burns and Pressey 1987; Galetto et al. 2010). In order to reduce the loss of sensory, texture, and cellular fluid during freezing, studies on enhancing the freezing rate and reducing the sizes of ice crystals have been extensive.

As a novel freezing technology, ultrasound-assisted immersion freezing (UF) has attracted considerable interest in recent years. Recently, the effects of ultrasound on food quality (Xin et al. 2014; Xu et al. 2015), ice crystal (Islam et al. 2015), and freezing parameters (Kiani and Sun 2011; Delgado et al. 2008) have been investigated. Several studies have reported that applying power ultrasound during immersion freezing was useful for inducing primary and secondary nucleation (Li and Sun 2002; Sun and Li 2003; Chow et al. 2003, 2005; Kiani and Sun 2011). This is mainly ascribed to acoustic cavitation, which can be divided into three stages: the formation, growth, and violent collapse of cavitation bubbles (Simal et al. 1998). Cavitation bubbles can act as ice nuclei to induce the primary nucleation: the collapse of cavitation bubbles can break pre-existing ice crystals into smaller ones, which then act as ice nuclei to promote secondary nucleation. Furthermore, power ultrasound can improve the convective heat transfer coefficient (Zheng and Sun 2006; Legay et al. 2011), because the implosion of cavitation bubbles near the solid-fluid interface disrupts the thermal and velocity boundary layers, resulting in the reduction of thermal resistance and the creation of microturbulence (Legay et al. 2011). Therefore, UF can effectively increase the freezing rate and minimize the size of ice crystals, thus maintaining the integrity of cell structures and improving the quality of frozen foods. However, ultrasound irradiation could result in some negative effects on plant tissue. Large amounts of hydroxyl radicals can be produced by ultrasonic cavitation during ultrasonic process, causing sonochemical oxidation of phenol (Serpone et al. 1992). Xu et al. (2015) indicated that samples treated with UF showed a significantly ($p < 0.05$) decrease in freezing time and a better preserved quality towards IF, as well as a less destructed microstructure. Similar results have been reported by Sun and Li (2003) for potato samples. Besides, several studies have also examined the effect of UF on various food materials, such as potato, red radish, apple, and strawberry (Islam et al. 2017). These studies have indicated that the application of power ultrasound during immersion freezing is extremely effective for reducing the freezing time and protecting the microstructure of tissues. Compared with normal immersion freezing (IF), the

freezing times using UF decreased by approximately 21.48% for strawberry (Cheng et al. 2014), 16.84% for radish (Xu et al. 2015), 14.29% for potato (Li and Sun 2002), and 8% for apple (Delgado et al. 2008).

However, the mechanisms causing the differences in freezing efficiencies are still unknown and have not been thoroughly explored. Being a mechanical wave, the energy of ultrasound continuously attenuates during the transmission process, and the ultrasonic attenuation coefficient differs in different media (Feng et al. 1999): in particular, severe ultrasonic attenuation occurs in air (Delgado and Sun 2011). The presence of voids in plant tissues, for example the air content of apples is about 20–25% (Khan and Vincent 1993; McClements and Gunasekaran 1997) and that of potato about 2% (Mizrach et al. 1989), causes scattering and absorption attenuation when ultrasound propagates in these tissues. It has also been reported that the ultrasonic attenuation coefficient increases as the void volumes of plant tissues increase (Liu et al. 2004; Ma and Liu 2012). Tamura et al. (2014) have also reported that ultrasonic transmission was hindered if the air content in the tissues was too high. Based on these studies, the void volume or air content within the plant tissues should have a remarkable influence on the effectiveness of UF.

Therefore, the main objective of the current study was to investigate the influence of voids in plant tissues on the effectiveness of UF. Apple, radish, and potato were chosen as food materials. The selection of these three plant samples (apple, radish, and potato) were due to their similar plant cell structure but with different levels of voids (high, medium, and low level of voids, respectively). Samples will be frozen using UF and IF, so that the effect of voids on the freezing time, firmness, drip loss, total calcium content, and total phenolic content of the samples can be evaluated.

Materials and Methods

Materials

The fresh apples (red Fuji), radishes (Nan Pan Zhou), and potatoes (Yueyin 85–38) used in the current study were purchased from a local supermarket in Guangzhou, China. They were first washed with tap water then cut into cylinders, 1.7 cm in diameter and 2.0 cm high, using a regular steel mold. These samples were then placed in plastic bags and kept in a refrigerator at 4 °C to achieve a uniform initial temperature until the freezing treatments were conducted. All the raw materials were used within 24 h of purchase.

Freezing Equipment

A laboratory scale UF system was set up for this study by the authors. Figure 1 shows the schematic diagram of the system. The freezing system consisted of the following three main parts: (1) an ultrasound bath, which was designed and manufactured Ningbo Scientz Biotechnology Co. Ltd. (Ningbo, China). The

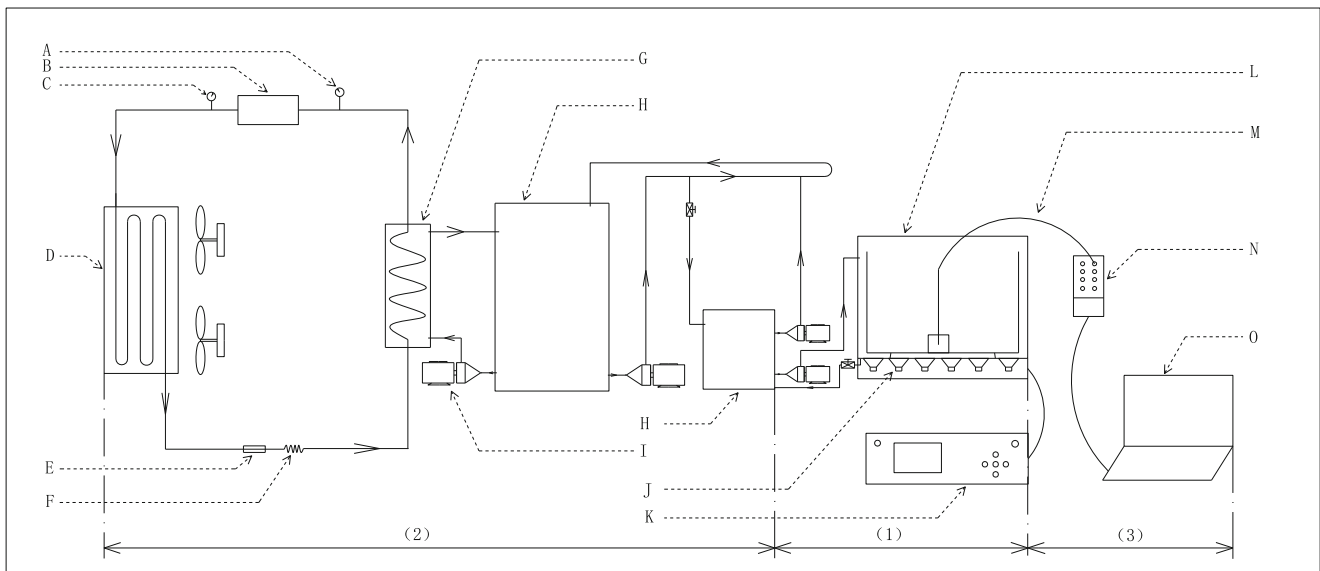


Fig. 1 Schematic diagram of the ultrasound-assisted freezing equipment (a low pressure gauge, b compressor, c high pressure gauge, d condenser, e filter, f expansion valve, g evaporator, h coolant tank, i pump, j

ultrasonic transducer, k ultrasonic generator, l freezing tank, m thermocouple, n data logger, o computer)

ultrasound bath consisted of an ultrasonic generator, eight ultrasonic transducers and a freezing tank; (2) a cooling system, which contained a refrigeration unit (Model LS-20 kW, Beijing BKP Technology Ltd., China) and a coolant circulator. Ethylene glycol solution (33%, v/v) was used as the coolant in the cooling system and three pumps kept the coolant circulating in the whole UF system; and (3) a temperature acquisition system, which included eight thermocouples (type-T, Omega Engineering Inc., Norwalk, CT, USA) 0.5 mm in diameter with an accuracy of ± 0.1 °C. These thermocouples were connected to a PC with a data logger (Model TC-08, OMEGA Engineering, Inc.) to acquire sample temperatures during freezing.

Experimental Procedure

The experimental procedure is shown in Fig. 2. The freezing treatments were IF and UF. During the freezing processes, the freezing tank was filled with 8.5-L coolant, which was maintained at a temperature of -18 ± 0.5 °C. When the coolant temperature was reduced to -18 °C, the cylindrical samples were removed from the refrigerator and immediately placed into the coolant. A type-T thermocouple was inserted into the geometric center of each sample to monitor the sample temperature. To minimize the effect of ultrasonic field fluctuation, all samples were placed at the same fixed locations in the freezing tank. The labels for the different freezing treatments of all samples were as follows: AIF (IF of apple), AUF (UF of apple), RIF (IF of radish), RUF (UF of radish), PIF (IF of potato), and PUF (UF of potato). For UF treatments, ultrasound waves (28 kHz, 0.62 W cm^{-2}) were applied when the sample center temperature reached -0.5 °C. To minimize the thermal effect of the ultrasound, the ultrasound was irradiated

intermittently at a cycle of 30 s on followed by 30 s off, with an accumulated exposure time of 2 min. The freezing process was completed when the sample center temperature reached -18 °C. After freezing, each sample was put into a polyethylene plastic bag and immediately transferred into a freezer at -18 °C for storage.

Analytical Methods

Measurement of Ultrasound Intensity

The power ultrasound was generated by the ultrasonic transducers and dissipated to the samples from the bottom of the freezing tank at a frequency of 28 kHz. During generation and transmission, due to attenuation, the actual power transmitted into the samples was lower than the power output. Therefore, it was necessary to determine the actual ultrasound intensity, which was measured using the calorimetric method (Raso et al. 1999). In this method, the temperature increase of water in a 2-mL centrifuge tube during the application of power ultrasound was recorded by a type-T thermocouple for 120 s. The dissipation power (P) was then calculated using the following equation:

$$P = MC_p \frac{dT}{dt} \quad (1)$$

where P is the dissipation power (W), M is the mass of water (kg), C_p is the specific heat capacity of water ($\text{kJ kg}^{-1} \text{K}^{-1}$), and dT/dt is the rate of temperature increase during ultrasound exposure (K s^{-1}). The actual dissipation power was calculated as 0.39 W when the ultrasonic generator operated at 70% of amplitude.

The ultrasound intensity (I) was then determined using:

$$I = \frac{P}{A} \quad (2)$$

where A is the cross-sectional area of the centrifuge tube (cm^2). The ultrasound intensity was calculated as 0.62 W cm^{-2} when the ultrasonic generator worked at 70% amplitude.

Measurement of Young's Modulus

Young's modulus measures the stiffness of a solid material, which was determined using a universal testing machine (Instron 5967, Instron Ltd., Norwood, MA, USA) in compression mode. In the test, samples were cut into cylinders (1.7 cm in diameter \times 2.5 cm in height), and the speed of the 100-mm flat probe was 5 mm/s. A force of 30 kN was used to cause a 40% compression. The force/compression curves were then recorded by a computer and the ratio of tensile stress to tensile strain was calculated as the Young's modulus. Four repetitions ($n = 4$) were carried out for each test and their average was reported.

Analysis of Microstructure

A confocal laser scanning microscopy (CLSM) (TCS-SPE, Leica Microsystems GmbH, Wetzlar, Germany) was used to observe the microstructure of samples (Cen et al. 2013). In the present study, two-dimensional (2-D) images were obtained at a selected confocal plane and the Leica Application Suite X Analysis software associated with the CLSM was used to analyze the images. For scanning, the tissue specimens (1.0 long \times 1.0 wide \times 0.1 cm thick) of fresh samples taken from about 1 cm beneath the surface were cut in the radial direction using a double-sided blade. The tissue specimens were then immediately immersed in a 0.1% Congo red solution (Tianjin Damao Chemical Reagent Factory, Tianjin, China) for 10 min. The specimens were then washed three times with distilled water before the CLSM with an excitation wavelength of 488 nm was used for microscopic imaging of the specimens.

Measurement of Firmness

The firmness of fresh samples and thawed samples was evaluated as described in Fernández-León et al. (2013). A TA-XT2i texture analyzer (Stable Micro Systems Ltd., Godalming, UK) with a cylindrical probe (2 mm in diameter) was used to measure the firmness of the supported samples with dimensions of 1.7 cm in diameter \times 2.5 cm in height. Before measurement, the texture analyzer was calibrated with a 1-kg weight. The compression mode was selected and the testing parameters of pre-speed, test-speed, post-speed, trigger

force, and deformation were set at 2.00 mm s^{-1} , 1.00 mm s^{-1} , 5.00 mm s^{-1} , 5.00 g, and 60%, respectively. The force-deformation curves were recorded using the software Texture Exponent 32 (Stable Micro Systems Ltd.) and the maximum compression force (N) was taken as firmness. Six replications ($n = 6$) were carried out for each test and the averaged values were reported.

Measurement of Water Content

During the test, samples were placed in an electrothermal drying box (DHG-9240A, Shanghai Yiheng Technology Co. Ltd., Shanghai, China) at 100°C for 1 h. After natural cooling, the samples were weighed on a piece of aluminum foil placed on a pre-tared electronic balance. The water content (W) of the samples was calculated as follows:

$$W = \frac{m_1 - m_2}{m_1 - m_3} \times 100\% \quad (3)$$

where m_1 (g) and m_2 (g) are the masses of the samples with aluminum foil before and after drying, respectively. m_3 (g) is the mass of the aluminum foil. Three parallel experiments were conducted and six replicates ($n = 6$) were carried out and the average was reported.

Measurement of Void Volume

The volume of the voids of sample was measured using methods based on Archimedes' principle (Dražeta et al. 2004). In the first step, the volume of a cylindrical sample was measured, and the sample volume (V) was determined by the following equation:

$$V = \pi r^2 h \quad (4)$$

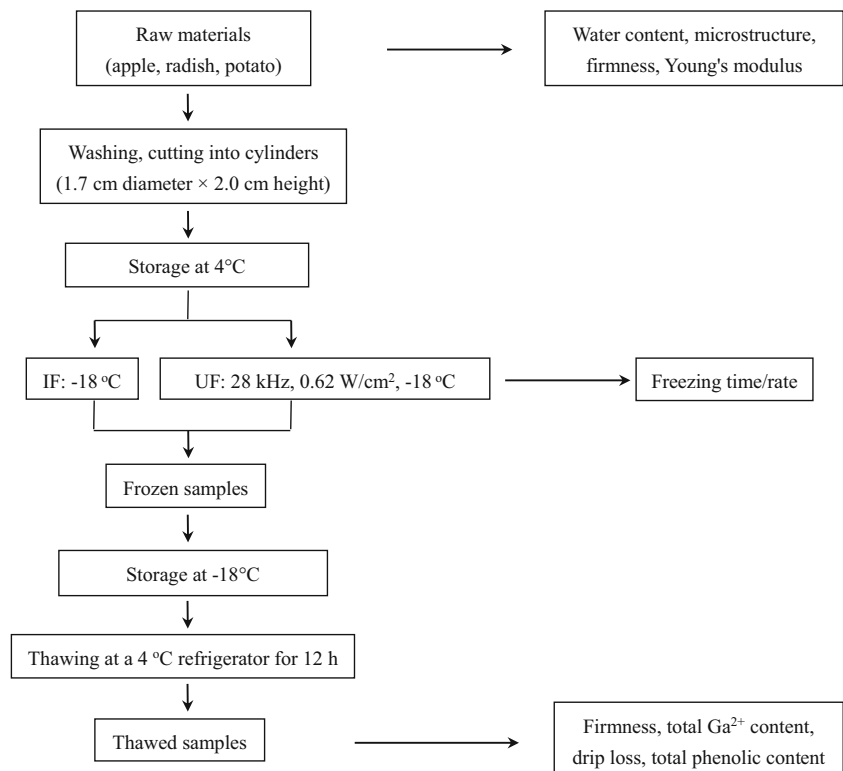
where r (cm) is the radius of the sample, and h (cm) is the height of the sample.

In the second step, the mass of the sample was measured in a water container resting on the pre-tared electronic balance. During the experiment, the sample masses before, W_1 (g), and after, W_2 (g), vacuum degassing under water were measured. The increase in sample mass was calculated based on the volume of air removed ($W = W_2 - W_1$). Then the percentage voids of the sample were expressed as:

$$O = \frac{W}{V} \times 100\% \quad (5)$$

where V (cm^3) is the volume of the sample, and O is the percentage voids of samples (g cm^{-3}). Three repetitions ($n = 3$) were carried out for each test and the averaged values were reported.

Fig. 2 Flow chart of experimental design. IF: normal immersion freezing; UF: ultrasound-assisted immersion freezing



Measurement of Drip Loss

After the freezing treatments, the frozen samples were placed in a refrigerator and thawed at 4 °C for 12 h. The masses before and after thawing were measured, and the drip loss (DL) was calculated by the equation below:

$$DL(\%) = \frac{m_0 - m_1}{m_0} \times 100 \quad (6)$$

where m_0 (g) is the mass of the sample before thawing, and m_1 (g) is the sample mass after thawing. Six parallel experiments were conducted and each test was repeated three times ($n = 3$) and their average was reported.

Measurement of Total Calcium Content

The total calcium content of sample was determined using the atomic absorption spectrophotometry (AAS) method described by Kawashima and Soares (2003) with slight modification. Fresh or thawed samples (5 g) were digested with 10 mL of 65% HNO_3 solution for 1 h, then put into a muffle furnace (SX-8-10, Taisite Instrument Co. Ltd., Tianjin, China) at 550 °C for 3.5 h. The residues were then transferred to a 100-mL volumetric flask and diluted with distilled water. At the same time, lanthanum nitrate and

nitric acid were added to final concentration of 0.5% ($v v^{-1}$) and 1% ($v v^{-1}$), respectively. An atomic absorption spectrometer (Z-2000, Hitachi Ltd., Tokyo, Japan) was used to determine the calcium content in the solution. Standard solution was prepared using CaCO_3 and the final concentration of lanthanum was kept at 0.5% ($v v^{-1}$). Three replications ($n = 3$) were carried out for each test.

Measurement of Total Phenolic Content

The total phenolic content was measured using the Folin-Ciocalteu (FC) method (Cheok et al. 2013) after extraction with aqueous ethanol. About 5 g samples and 50 mL of 15% ethanol solution were mixed together in a beaker then homogenized at 16,000 rpm for 2 min with a homogenizer. The mixture was extracted in a 30 °C water bath for 1 h. The mixture was then centrifuged at $10,013 \times g$ for 20 min at 4 °C using a refrigerated centrifuge (H2050, Xiangyi Centrifuge Equipment Ltd., Hunan, China), the supernatant was decanted into a beaker, and the precipitate was extracted again. Finally, the supernatants were mixed and stored at -18 °C for the following determination. The extract was diluted by a factor of 4 before the test. Then, 2.00-mL diluted extraction was transferred into a test tube and mixed thoroughly with 1.00 mL of 0.2 mol/L FC reagent (2 N, Sigma-Aldrich, St. Louis, MO, USA). After shaking for 3 min, 2.00 mL of NaCO_3 solution (15%, w/v) was added and finally made up

to 10 mL with distilled water. The mixture was kept in the dark for 30 min before measuring its absorbance in a UV-visible spectrophotometer (L5S, Inesa Analytical Instrument Co. Ltd., Shanghai, China) at 765 nm. The total phenolic content was expressed in mg of gallic acid equivalents (GAE) per 100 g fresh weight. A calibration curve ($y = 0.035x - a0.006$, $R^2 = 0.996$) was established for standard gallic acid. Three replications ($n = 3$) were carried out for each test.

Statistical Analysis

Data were analyzed using SPSS software (Version 20, 2011, IBM SPSS Statistics for Windows, Armonk, NY, USA), and significant differences between sample means were evaluated using one-way variance analysis (ANOVA, Tukey's test procedure, 95% significance level).

Results and Discussion

Ultrasonic Attenuation

Density (ρ), sound velocity (c), and attenuation coefficient (α) are normally used for describing the acoustic characteristics of homogeneous materials, which are affected by the specific acoustic impedance (Z), depicted below (Feng et al. 1999):

$$Z = \rho \times c \quad (7)$$

The specific acoustic impedance and the attenuation coefficient can then be used to characterize the acoustic property of a material.

The velocity of the ultrasonic longitudinal wave, c , in an infinite medium can be expressed as:

$$c = \sqrt{\frac{E(1-\sigma)}{\rho(1+\sigma)(1-2\sigma)}} \quad (8)$$

where E is the Young's modulus and σ is the Poisson's ratio.

Therefore, the specific acoustic impedance can be calculated as:

$$Z = \sqrt{\frac{E\rho(1-\sigma)}{(1+\sigma)(1-2\sigma)}} \quad (9)$$

The Young's modulus for the apple, radish, and potato samples listed in Table 1 shows that that for apple was the lowest. The density of the potatoes, radishes, and apples were 0.99, 0.90, and 0.78 g cm⁻³, respectively. As Poisson's ratio is a constant, the specific acoustic impedance of apple was thus

the lowest. Figure 3 shows the confocal laser scanning microscopic (CLSM) images of the flesh tissue specimens. After analyzing the CLSM images using Leica Application Suite X Analysis software, the volume percentage of voids in the different samples, shown in Table 1, revealed significant differences in voids between the three different samples ($p < 0.05$). It has been reported that the attenuation coefficients of ultrasound (1 MHz) were 0.002 dB/cm in 0.9% physiological saline, while 12.0 dB/cm in air (Feng et al. 1999). Therefore, higher percentage volume voids would result in a higher air content, hence a greater degree of ultrasonic attenuation.

Freezing Curves

During IF and UF experiments, temperatures in the geometric center of the samples were recorded, and Fig. 4 shows the freezing curves. To help with comparison in the current study, a total freezing time for the temperature at the sample center was defined as spanning from 4 to -15 °C and a phase transition time spanning from 0 to -5 °C when most crystallization took place. It was noted that the total freezing time for the radish and potato samples was significantly different ($p < 0.05$) when ultrasound was applied (Fig. 4b). Compared with IF, the total freezing time for apple, radish, and potato in UF decreased by 5.40, 17.75, and 26.32%, respectively. The freezing rate was thus greatly improved by the application of ultrasound, ascribed to the improvement of heat transfer efficiency and the promotion of nucleation (Li and Sun 2002; Sigfusson et al. 2004).

Recently, the capacity of ultrasound to promote nucleation in liquid (deionized water and sucrose solution) (Kiani et al. 2011), solid model foods (agar gel) (Kiani et al. 2012), and vegetable foods (potato and strawberry) (Comandini et al. 2013; Cheng et al. 2014) have been studied, indicating that ultrasound was capable of promoting nucleation. Three theories have been commonly cited to illustrate the mechanism of accelerating freezing by ultrasound. Firstly, the high pressure (5 GPa) generated by the cavitation bubbles leads to a higher degree of supercooling (Hickling 1965) as the driving force of nucleation (Inada et al. 2001). Secondly, the effect of microstreaming can reduce the heat transfer resistance near the solid-liquid interface thus enhancing heat transfer (Li and Sun 2002; Legay et al. 2011; Zheng and Sun 2006). Thirdly, cavitation bubbles can act as ice nuclei to induce the primary nucleation (Chow et al. 2003). Furthermore, pre-existing dendritic ice clusters can be broken into small crystal fragments, which act as new ice nuclei to promote secondary nucleation (Chow et al. 2005). The phase transition times of the three different samples are also shown in Fig. 4b. Compared with IF, the phase transition times in UF decreased by 6.36, 20.09, and 28.55% for apple, radish, and potato samples, respectively. Therefore, UF shortened the duration of phase transition mainly by promoting the formation of ice nuclei,

Table 1 Basic parameters determined for the three different plant samples

Sample	Voids (%)	Young's modulus (MPa)	Water content (%)	Firmness (N)
Apple (A)	25.68 ± 0.011 ^c	3.28 ± 0.229 ^a	84.25 ± 0.001 ^b	7.74 ± 0.429 ^a
Radish (R)	11.39 ± 0.004 ^b	4.42 ± 0.084 ^b	95.51 ± 0.001 ^c	11.67 ± 0.235 ^b
Potato (P)	7.81 ± 0.008 ^a	3.98 ± 0.137 ^{ab}	76.09 ± 0.005 ^a	16.84 ± 0.852 ^c

Mean values within columns with different superscript letters are significantly different ($p < 0.05$). All values are mean ± standard deviation

thus improving the freezing efficiency. Similar results have been reported by Li and Sun (2002) for potato samples.

However, the total freezing time and phase transition time were not significantly ($p > 0.05$) reduced in apple samples, which might be due to the more and larger voids within apple tissue (Fig. 3), resulting in severe ultrasonic attenuation. Figure 4c shows the relationship between the volume percentage of voids and the percentage total freezing time reduction due to UF for the three kinds of samples. This data could be fitted to a power function as $y = 0.018x^{-1.057}$ ($R^2 = 0.994$), where y is the total freezing time reduction (%) due to UF and x is the volume of voids (%).

Firmness of Thawed Samples

The firmness, an index of the texture, of the thawed samples treated by IF and UF and that in fresh samples is compared in Fig. 5a. This showed that the firmness of the thawed samples decreased significantly ($p < 0.05$), which could be attributed to the crystallization of ice in tissues causing mechanical damage to the natural cellular structure (Sanz et al. 1999; Fernández et al. 2006). The difference of intracellular and extracellular fluid concentration (Fennema 1973), as well as the partial vapor pressure difference between water and ice crystals

(Sahagian and Goff 1996), both promoted the growth of extracellular ice crystals. Fresh plant tissues having a higher moisture content are more likely to form large ice crystals during the freezing process (Xin et al. 2014). It has been reported that the texture of frozen food after thawing is greatly affected by the size and distribution of ice crystals, which are closely related to the freezing rate (Petzold and Aguilera 2009). However, some research showed that calcium treatment could also help improve the firmness of frozen samples (Cosgrove 2005; Xu et al. 2015).

It has been reported that the cell walls were not be damaged by applying power ultrasound (Sun and Li 2003; Fernandes et al. 2009), whereas the growth of ice crystals would lead to their rupture (Chevalier et al. 2000). Hu et al. (2013) and Islam et al. (2014) have reported that the application of UF produced many small ice crystals in food materials. As can be seen from Fig. 5a, compared with IF, the loss of firmness of thawed apple, radish, and potato after UF process was improved by 5.58, 6.16, and 12.50%, respectively. These improvements could probably be attributed to the increase in freezing rate during the UF process (Fig. 4a, b), which resulted in the formation of evenly distributed small ice crystals, thus minimizing the possibility of mechanical damage. Especially, firmness in potato after IF decreased by approximately 41.39%

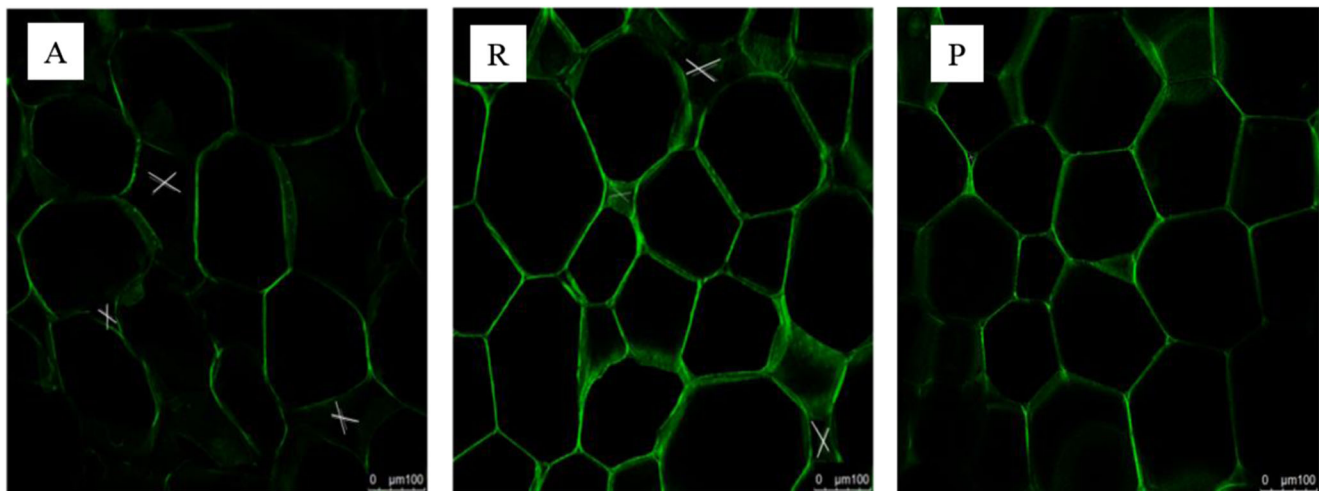


Fig. 3 Confocal laser scanning microscopic images of flesh tissue specimens 1 cm beneath the skin in the radial direction for three different plants. A, R, and P represent apple, radish, and potato, respectively, “X” represent void

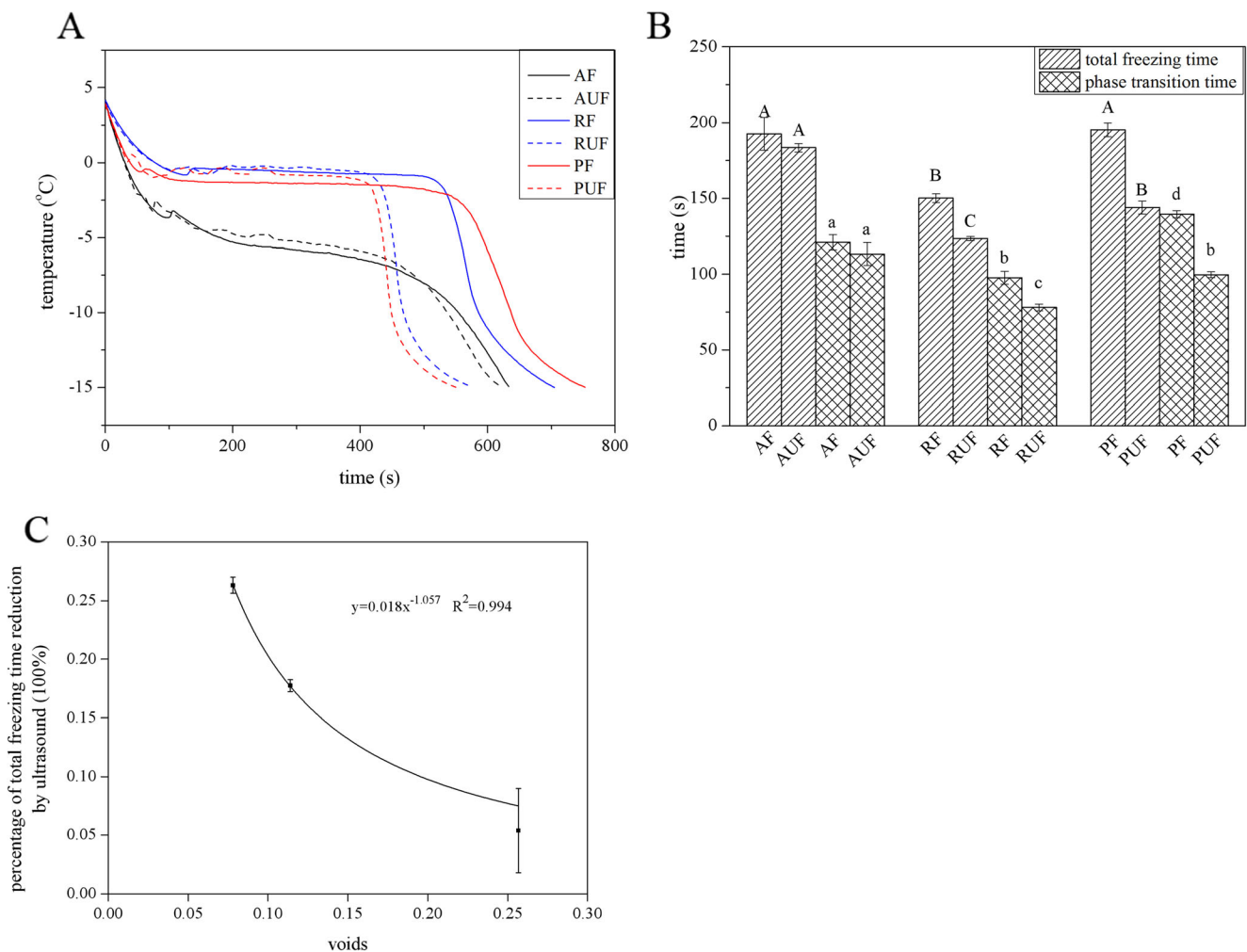


Fig. 4 Effects of voids in plant tissues on freezing efficiency during UF. **a** Freezing curves of three kinds of materials in two different freezing methods. **b** Total freezing time and phase transition time (s) for different freezing methods. **c** Relationship between the percentage of total freezing time reduction (%) and the volume of voids (%). AIF, AUF, RIF, RUF, PIF, and PUF represent normal immersion freezing of

apple, ultrasound-assisted immersion freezing of apple, normal immersion freezing of radish, ultrasound-assisted immersion freezing of radish, normal immersion freezing of potato, and ultrasound-assisted immersion freezing of potato, respectively. Mean values for columns of the same treatment with different letters (uppercase or lowercase) are significantly different ($p < 0.05$). Error bars show \pm standard deviation

compared to fresh samples, while only 14.96% after UF process, which could be attributed to the fact that potatoes have the lowest voids (Table 1) among the three samples, thus a lower ultrasound attenuation.

Drip Loss

Drip loss is one of the most crucial indices to evaluate the quality of frozen samples. The drip loss for the three different samples with IF and UF treatments is shown in Fig. 5b, indicating that UF significantly limited the decrease in the drip loss of radish and potato samples compared with IF ($p < 0.05$), while the differences for drip loss of apple samples were not significant. Noticeably, the variation of drip losses in IF and UF were not significantly different for all the plant tissues, and were highly consistent with the freezing rate (Fig. 4b) and

firmness (Fig. 5a). Therefore, it could be concluded that the decreases in drip loss during thawing were mainly due to the formation of smaller ice crystals during the freezing process, because the dense structure of potato and radish was beneficial for ultrasound transmission. In addition, the maintenance of calcium (Fig. 5c) might also play an important role in maintaining the integrity of the cell wall, contributing to the reduction in drip loss. However, the apples used in the current study contained 25.68% voids (Table 1), and air in these intercellular spaces could have caused serious attenuation of ultrasound and thus lowering the effectiveness of ultrasonic cavitation. Therefore, the cell wall could not be better protected during thawing, causing serious drip loss from the plant tissue, so no obvious decrease in drip loss for the apple samples was observed. Besides, the water content of apples reached 84.25% as indicated in Table 1. The drip loss of the apple samples was

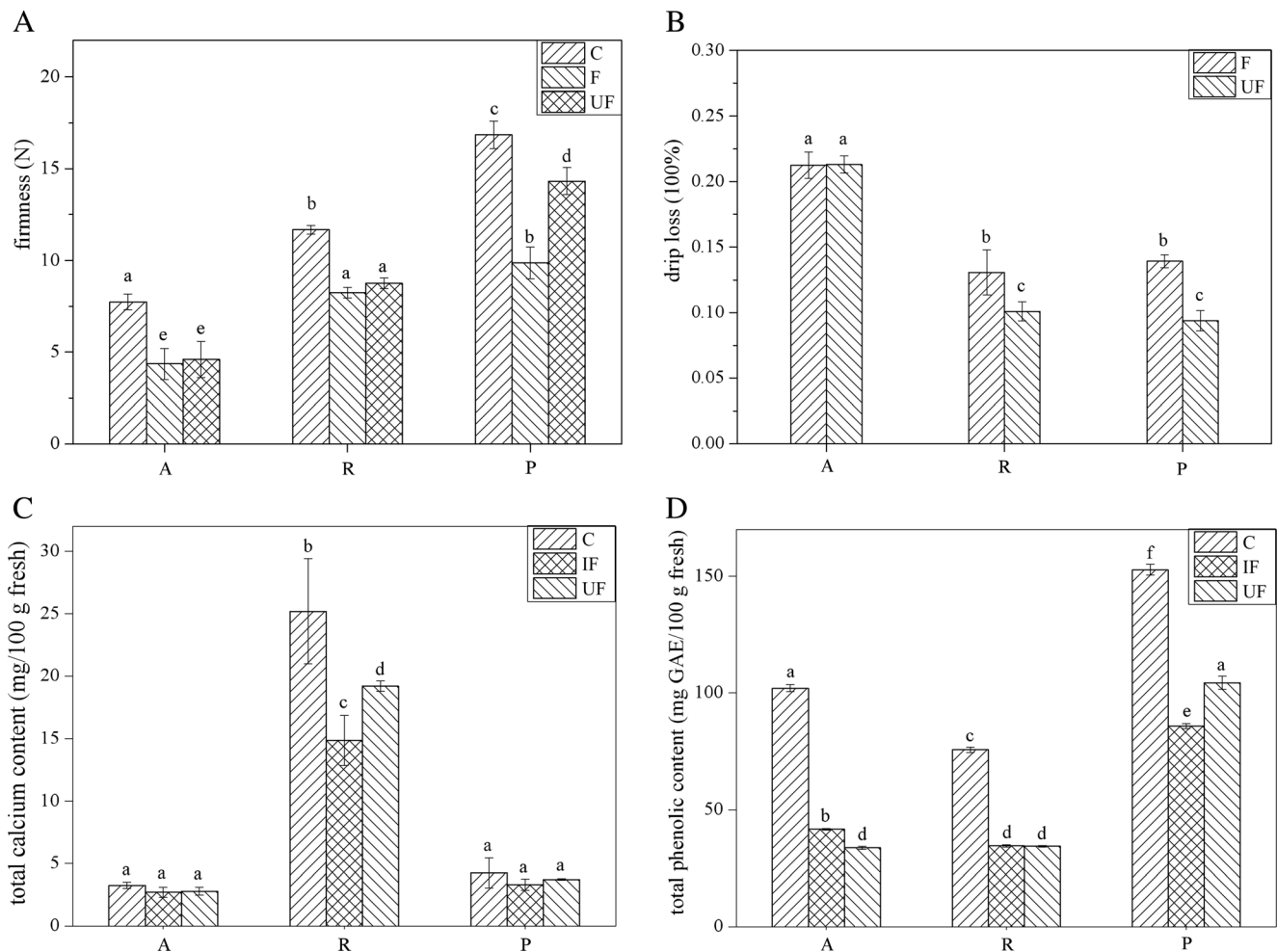


Fig. 5 Effects of voids in plant tissues on the quality attributes of frozen products during UF. **a** firmness. **b** Drip loss. **c** Total calcium content. **d** Total phenolic content. A, R, and P represent apple, radish, and potato, respectively. C, IF, and UF represent fresh sample, normal immersion

freezing, and ultrasound-assisted immersion freezing, respectively. Mean values for columns of the same tissue sample with different letters are significantly different ($p < 0.05$). Error bars show \pm standard deviation

the highest of the three different samples, mainly due to the high water content and percentage voids in apple tissue.

Total Calcium Content

Due to the fact that calcium bound in the cell wall plays a major role in protecting its integrity, calcium pre-treatments are always applied to retard the softening of harvested vegetables and fruits (Galletto et al. 2010; Xin et al. 2014). Additionally, the differences in calcium content of plant tissues after thawing can reflect the degree of tissue damage to some extent (Alonso et al. 1995). As can be seen from Fig. 5c, the total calcium content in thawed samples was lower than that of fresh samples. This was because the generation of ice crystals could result in possible mechanical damage to the cells, causing the release of bound calcium as free calcium (Alonso et al. 1995) that would be eventually be lost with the drip. Similar results have been

reported by Galletto et al. (2010) for strawberry, Xin et al. (2014) for broccoli, and Xu et al. (2015) for red radish.

The experimental data showed that the total calcium content in fresh radish was the highest (25.19 mg/100 g), while those in fresh potato and apple were 4.24 and 3.25 mg/100 g, respectively (Fig. 5c). Compared with fresh samples, the total calcium content was significantly ($p < 0.05$) decreased by 41.01% for radish after IF and 23.78% after UF, while no significant differences ($p > 0.05$) were observed in the thawed potato and apple samples, which were due to low contents of calcium in fresh potato and apple. In general, UF samples showed significantly ($p < 0.05$) higher ratio of total calcium contents than IF samples, which indicated that the application of UF could maintain the calcium content to a certain degree, especially evident in plant tissues with high calcium content, possibly due to the shorter freezing time

(Fig. 4a) and the formation of smaller ice crystals in UF treatment.

Total Phenolic Content

The total phenolic contents of fresh and thawed samples are shown in Fig. 5d. Obviously, compared with the fresh samples, the total phenolic contents of the three different samples were significantly ($p < 0.05$) reduced after freezing and thawing. This might have been caused for two reasons: (1) plenty of hydroxyl radicals (OH^\cdot) were generated due to the ultrasonic cavitation, and the OH^\cdot had strongly oxidized part of the phenolic contents (Kidak and Ince 2006; Serpone et al. 1992) and (2) ice crystals formed during the freezing process might have damaged the cell structure (Fernández et al. 2006; Sanz et al. 1999), thus part of the phenolic content was lost during thawing.

Compared with fresh samples, IF samples lost 59.20% of total phenolic contents in apple, 54.66% in reddish, and 43.81% in potato, compared with 66.92, 54.41, and 31.69%, respectively, in UF samples. This indicated that UF could significantly ($p < 0.05$) limit the decrease of the total phenolic content in potato, due to a lower voids volume in potato tissue (Table 1), which could effectively reduce the ultrasonic attenuation, thus limiting the drip loss. The amount of total phenolic loss by decreasing drip loss was much greater than that lost due to OH^\cdot oxidation, which might account for the reason why no significant difference existed in radish between IF and UF. In contrast, high percentage volume of voids in apple led to the most of the drip loss, as well as the thermal effect of ultrasound and the oxidation caused by hydroxyl radicals (Kidak and Ince 2006), causing a significant decrease in total phenol content in apple tissue under UF treatment.

Conclusions

The effect of voids on the freezing efficiency of apple, radish, and potato samples frozen by UF has been investigated in terms of the freezing time, firmness, drip loss, total calcium, and total phenolic content of samples. The results showed that the volume of voids had a great impact on ultrasound transmission. The application of ultrasound during immersion freezing mainly promoted the generation of ice nuclei, leading to the shortening of the phase transition time and the improvement of the freezing rate. Therefore, ultrasound irradiation should be applied during the phase transition stage. Additionally, the firmness, total calcium, and total phenolic content of the frozen samples were better preserved and the drip loss was reduced under low void volume conditions. These results have shown that the fewer

the voids in plant tissues, the higher the effectiveness of ultrasound, which could possibly enhance the quality of the frozen product. However, compared with apple and radish, a shorter freezing time was needed and a better cell structure was preserved in potato tissues by applying ultrasound. The percentage of total freezing time reduction was a power function of the volume percentage of voids within the samples. Different void volumes and Young's modulus of the apple, radish, and potato tissues resulted in different specific acoustic impedances and ultrasonic attenuation coefficients. This seriously affected the effectiveness of ultrasound irradiation during the immersion freezing process. These findings suggest that UF should be applied to food materials with have a highly dense structure.

Funding Information The authors are grateful to the National Key R&D Program of China (2017YFD0400404) for its support. This research was also supported by the Collaborative Innovation Major Special Projects of Guangzhou City (201604020057), the Agricultural Development and Rural Work of Guangdong Province (2017LM4173), the International and Hong Kong–Macau–Taiwan Collaborative Innovation Platform of Guangdong Province on Intelligent Food Quality Control and Process Technology & Equipment (2015KGJHZ001), the Guangdong Provincial R & D Centre for the Modern Agricultural Industry on Non-Destructive Detection and Intensive Processing of Agricultural Products, the Common Technical Innovation Team of Guangdong Province on Preservation and Logistics of Agricultural Products (2016LM2154), and the Innovation Centre of Guangdong Province for Modern Agricultural Science and Technology on Intelligent Sensing and Precision Control of Agricultural Product Qualities.

References

- Alonso, J., Rodriguez, T., & Canet, W. (1995). Effect of calcium pretreatments on the texture of frozen cherries. Role of pectinesterase in the changes in the pectic materials. *Journal of Agricultural and Food Chemistry*, 43(4), 1011–1016.
- Alvarez, M. D., Fernandez, C., & Canet, W. (2005). Effect of freezing/thawing conditions and long-term frozen storage on the quality of mashed potatoes. *Journal of the Science of Food and Agriculture*, 85(14), 2327–2340.
- Burns, J. K., & Pressey, R. (1987). Ca^{2+} in cell walls of ripening tomato and peach. *Journal of the American Society for Horticultural Science*, 112(5), 783–787.
- Cen, H., Lu, R., Mendoza, F., & Beaudry, R. M. (2013). Relationship of the optical absorption and scattering properties with mechanical and structural properties of apple tissue. *Postharvest Biology and Technology*, 85, 30–38.
- Cheng, X., Zhang, M., Adhikari, B., Islam, M. N., & Xu, B. (2014). Effect of ultrasound irradiation on some freezing parameters of ultrasound-assisted immersion freezing of strawberries. *International Journal of Refrigeration*, 44, 49–55.
- Cheng, J.-H., Sun, D.-W., & Pu, H. (2016). Combining the genetic algorithm and successive projection algorithm for the selection of feature wavelengths to evaluate exudative characteristics in frozen-thawed fish muscle. *Food Chemistry*, 197, 855–863.
- Cheng, L., Sun, D.-W., Zhu, Z., & Zhang, Z. (2017). Emerging techniques for assisting and accelerating food freezing processes: A review of recent research progresses. *Critical Reviews in Food Science and Nutrition*, 57, 769–781.

- Cheng, W., Sun, D.-W., Pu, H., & Wei, Q. (2018). Characterization of myofibrils cold structural deformation degrees of frozen pork using hyperspectral imaging coupled with spectral angle mapping algorithm. *Food Chemistry*, 239, 1001–1008.
- Cheok, C. Y., Chin, N. L., Yusof, Y. A., & Talib, R. A. (2013). Optimization of total monomeric anthocyanin (TMA) and total phenolic content (TPC) extractions from mangosteen (*Garcinia mangostana* Linn.) hull using ultrasonic treatments. *Industrial Crops and Products*, 50, 1–7.
- Chevalier, D., Bail, A. L., & Ghoul, M. (2000). Freezing and ice crystals formed in a cylindrical food model: part II. Comparison between freezing at atmospheric pressure and pressure-shift freezing. *Journal of Food Engineering*, 46(4), 287–293.
- Chow, R., Blindt, R., Chivers, R., & Povey, M. J. W. (2003). The sonocrystallisation of ice in sucrose solutions: primary and secondary nucleation. *Ultrasonics*, 41(8), 595–604.
- Chow, R., Blindt, R., Chivers, R., & Povey, M. J. W. (2005). A study on the primary and secondary nucleation of ice by power ultrasound. *Ultrasonics*, 43(4), 227–230.
- Comandini, P., Blanda, G., Sotocaballero, M. C., Sala, V., Tylewicz, U., Mujicapaz, H., Fragosó, A. V., & Toschi, T. G. (2013). Effects of power ultrasound on immersion freezing parameters of potatoes. *Innovative Food Science & Emerging Technologies*, 18, 120–125.
- Cosgrove, D. J. (2005). Growth of the plant cell wall. *Nature Reviews Molecular Cell Biology*, 6(11), 850–861.
- Delgado, A., & Sun, D.-W. (2011). Ultrasound-assisted freezing. In: *Ultrasound technologies for food and bioprocessing*. (pp. 495–509): Springer.
- Delgado, A. E., Zheng, L., & Sun, D.-W. (2008). Influence of ultrasound on freezing rate of immersion-frozen apples. *Food and Bioprocess Technology*, 2(3), 263–270.
- Desmond, E. M., Kenny, T. A., Ward, P., & Sun, D.-W. (2000). Effect of rapid and conventional cooling methods on the quality of cooked ham joints. *Meat Science*, 56, 271–277.
- Dražeta, L., Lang, A., Hall, A. J., Volz, R. K., & Jameson, P. E. (2004). Air volume measurement of ‘Braeburn’ apple fruit. *Journal of Experimental Botany*, 55(399), 1061–1069.
- Feng, N., Yao, J., & Guan, L. (1999). *Ultrasonics handbook*. Nanjing: Nan Jing University Press.
- Fennema, O. (1973). In M. Dekker (Ed.), *Nature of the freezing process. Low temperature preservation of foods and living matter* (pp. 151–222). New York.
- Fernández-León, M., Fernández-León, A., Lozano, M., Ayuso, M., & González-Gómez, D. (2013). Altered commercial controlled atmosphere storage conditions for ‘Parhenon’ broccoli plants (*Brassica oleracea* L. var. *italica*). Influence on the outer quality parameters and on the health-promoting compounds. *LWT - Food Science and Technology*, 50(2), 665–672.
- Fernández, P., Otero, L., Guignon, B., & Sanz, P. (2006). High-pressure shift freezing versus high-pressure assisted freezing: effects on the microstructure of a food model. *Food Hydrocolloids*, 20(4), 510–522.
- Fernandes, F. A. N., Gallao, M. I., & Rodrigues, S. (2009). Effect of osmosis and ultrasound on pineapple cell tissue structure during dehydration. *Journal of Food Engineering*, 90(2), 186–190.
- Góral, D., & Kluza, F. (2009). Cutting test application to general assessment of vegetable texture changes caused by freezing. *Journal of Food Engineering*, 95(2), 346–351.
- Galetto, C. D., Verdini, R. A., Zorrilla, S. E., & Rubiolo, A. C. (2010). Freezing of strawberries by immersion in CaCl₂ solutions. *Food Chemistry*, 123(2), 243–248.
- Hickling, R. (1965). Nucleation of freezing by cavity collapse and its relation to cavitation damage. *Nature*, 206(4987), 915–917.
- Hu, S., Liu, G., Li, L., Li, Z., & Hou, Y. (2013). An improvement in the immersion freezing process for frozen dough via ultrasound irradiation. *Journal of Food Engineering*, 114(1), 22–28.
- Hu, Z. H., & Sun, D.-W. (2000). CFD simulation of heat and moisture transfer for predicting cooling rate and weight loss of cooked ham during air-blast chilling process. *Journal of Food Engineering*, 46, 189–197.
- Inada, T., Zhang, X., Yabe, A., & Kozawa, Y. (2001). Active control of phase change from supercooled water to ice by ultrasonic vibration 1. Control of freezing temperature. *International Journal of Heat and Mass Transfer*, 44(23), 4523–4531.
- Islam, M. N., Zhang, M., Adhikari, B., Xinfeng, C., & Xu, B. (2014). The effect of ultrasound-assisted immersion freezing on selected physicochemical properties of mushrooms. *International Journal of Refrigeration*, 42, 121–133.
- Islam, M. N., Zhang, M., Fang, Z., & Sun, J. (2015). Direct contact ultrasound assisted freezing of mushroom (*Agaricus bisporus*): growth and size distribution of ice crystals. *International Journal of Refrigeration*, 57, 46–53.
- Islam, M. N., Zhang, M., & Adhikari, B. (2017). Ultrasound-assisted freezing of fruits and vegetables: design, development, and applications. In *Global food security and wellness* (pp. 457–487). New York: Springer.
- Kawashima, L. M., & Soares, L. M. V. (2003). Mineral profile of raw and cooked leafy vegetables consumed in southern Brazil. *Journal of Food Composition and Analysis*, 16(5), 605–611.
- Khan, A. A., & Vincent, J. F. V. (1993). Compressive stiffness and fracture properties of apple and potato parenchyma. *Journal of Texture Studies*, 24(4), 423–435.
- Kiani, H., & Sun, D.-W. (2011). Water crystallization and its importance to freezing of foods: a review. *Trends in Food Science and Technology*, 22(8), 407–426.
- Kiani, H., Sun, D.-W., Delgado, A. E., & Zhang, Z. (2012). Investigation of the effect of power ultrasound on the nucleation of water during freezing of agar gel samples in tubing vials. *Ultrasonics Sonochemistry*, 19(3), 576–581.
- Kiani, H., Zhang, Z., Delgado, A. E., & Sun, D.-W. (2011). Ultrasound assisted nucleation of some liquid and solid model foods during freezing. *Food Research International*, 44(9), 2915–2921.
- Kidak, R., & Ince, N. H. (2006). Ultrasonic destruction of phenol and substituted phenols: a review of current research. *Ultrasonics Sonochemistry*, 13(3), 195–199.
- Koushki, M. R., Mohammadi, M., Javadi, N. H. S., Komeily, R., Moslemy, M., Ahmadian, F. S., & Zali, H. (2013). The influence of freezing conditions on the organoleptic attributes of Iranian leafy vegetable foods. *Journal of Paramedical Sciences*, 4(Supplement), 42–46.
- Legay, M., Gondrexon, N., Person, S. L., Boldo, P., & Bontemps, A. (2011). Enhancement of heat transfer by ultrasound: review and recent advances. *International Journal of Chemical Engineering*, 2011, 1–17.
- Li, B., & Sun, D.-W. (2002). Effect of power ultrasound on freezing rate during immersion freezing of potatoes. *Journal of Food Engineering*, 55(3), 277–282.
- Liu, L., Lu, M., Zhang, B., Wang, D., Zheng, Y., & Zhang, C. (2004). Effects of porosity on the ultrasonic absorption coefficient and mechanical strength of carbon/epoxy composites. *Acta Materialia Sinica*, 21(5), 116–121.
- Ma, J., Pu, H., Sun, D.-W., Gao, W., Qu, J.-H., & Ma, K.-Y. (2015). Application of Vis-NIR hyperspectral imaging in classification between fresh and frozen-thawed pork Longissimus Dorsi muscles. *International Journal of Refrigeration-Revue Internationale Du Froid*, 50, 10–18.
- Ma, J., Sun, D.-W., Qu, J.-H., & Pu, H. (2017). Prediction of textural changes in grass carp fillets as affected by vacuum freeze drying using hyperspectral imaging based on integrated group wavelengths. *LWT-Food Science and Technology*, 82, 377–385.

- Ma, W., & Liu, F. (2012). Effect of porosity on the attenuation coefficient and mechanical properties of glass fiber reinforced composites. *Acta Materialia Compositae Sinica*, 29(5), 69–75.
- McClements, D. J., & Gunasekaran, S. (1997). Ultrasonic characterization of foods and drinks: principles, methods, and applications. *Critical Reviews in Food Science and Nutrition*, 37(1), 1–46.
- McDonald, K., & Sun, D.-W. (2001). The formation of pores and their effects in a cooked beef product on the efficiency of vacuum cooling. *Journal of Food Engineering*, 47, 175–183.
- McDonald, K., Sun, D.-W., & Kenny, T. (2001). The effect of injection level on the quality of a rapid vacuum cooled cooked beef product. *Journal of Food Engineering*, 47, 139–147.
- Mizrach, A., Galili, N., & Rosenhouse, G. (1989). Determination of fruit and vegetable properties by ultrasonic excitation. *Transactions of the ASABE*, 32(6), 2053–2058.
- Petzold, G., & Aguilera, J. M. (2009). Ice morphology: fundamentals and technological applications in foods. *Food Biophysics*, 4(4), 378–396.
- Pu, H., Sun, D.-W., Ma, J., & Cheng, J.-H. (2015). Classification of fresh and frozen-thawed pork muscles using visible and near infrared hyperspectral imaging and textural analysis. *Meat Science*, 99, 81–88.
- Pu, Y.-Y., & Sun, D.-W. (2016). Prediction of moisture content uniformity of microwave-vacuum dried mangoes as affected by different shapes using NIR hyperspectral imaging. *Innovative Food Science & Emerging Technologies*, 33, 348–356.
- Pu, Y.-Y., & Sun, D.-W. (2017). Combined hot-air and microwave-vacuum drying for improving drying uniformity of mango slices based on hyperspectral imaging visualisation of moisture content distribution. *Biosystems Engineering*, 156, 108–119.
- Qu, J.-H., Sun, D.-W., Cheng, J.-H., & Pu, H. (2017a). Mapping moisture contents in grass carp (*Ctenopharyngodon idella*) slices under different freeze drying periods by Vis-NIR hyperspectral imaging. *LWT-Food Science and Technology*, 75, 529–536.
- Qu, J.-H., Sun, D.-W., Cheng, J.-H., & Pu, H. (2017b). Mapping moisture contents in grass carp (*Ctenopharyngodon idella*) slices under different freeze drying periods by Vis-NIR hyperspectral imaging. *LWT-Food Science and Technology*, 75, 529–536.
- Raso, J., Manas, P., Pagan, R., & Sala, F. J. (1999). Influence of different factors on the output power transferred into medium by ultrasound. *Ultrasonics Sonochemistry*, 5(4), 157–162.
- Sahagian, M. E., & Goff, H. D. (1996). *Fundamental aspects of the freezing process*. *Food Science and Technology* (pp. 1–50). New York: Marcel Dekker.
- Sanz, P. D., De Elvira, C., Martino, M. N., Zaritzky, N. E., Otero, L., & Carrasco, J. (1999). Freezing rate simulation as an aid to reducing crystallization damage in foods. *Meat Science*, 52(3), 275–278.
- Serpone, N., Terzian, R. A., Colarusso, P., Minero, C., Pelizzetti, E., & Hidaka, H. (1992). Sonochemical oxidation of phenol and three of its intermediate products in aqueous media : catechol, hydroquinone, and benzoquinone. Kinetic and mechanistic aspects. *Research on Chemical Intermediates*, 18(2), 183–202.
- Sigfusson, H., Ziegler, G. R., & Coupland, J. N. (2004). Ultrasonic monitoring of food freezing. *Journal of Food Engineering*, 62(3), 263–269.
- Simal, S., Benedito, J., Sanchez, E. S., & Rossello, C. (1998). Use of ultrasound to increase mass transport rates during osmotic dehydration. *Journal of Food Engineering*, 36(3), 323–336.
- Sun, D.-W., & Woods, J. L. (1993). The moisture-content relative-humidity equilibrium relationship of wheat - a review. *Drying Technology*, 11, 1523–1551.
- Sun, D.-W., & Woods, J. L. (1994a). Low-temperature moisture transfer characteristics of barley - thin-layer models and equilibrium isotherms. 59, 273–283.
- Sun, D.-W., & Woods, J. L. (1994b). Low-temperature moisture transfer characteristics of wheat in thin-layers. *Transactions of the ASAE*, 37, 1919–1926.
- Sun, D.-W., & Woods, J. L. (1994c). The selection of sorption isotherm equations for wheat-based on the fitting of available data. *Journal of Stored Products Research*, 30, 27–43.
- Sun, D.-W., & Eames, I. W. (1996). Performance characteristics of HCFC-123 ejector refrigeration cycles. *International Journal of Energy Research*, 20, 871–885.
- Sun, D.-W. (1999). Comparison and selection of EMC ERH isotherm equations for rice. *Journal of Stored Products Research*, 35, 249–264.
- Sun, D.-W., & Li, B. (2003). Microstructural change of potato tissues frozen by ultrasound-assisted immersion freezing. *Journal of Food Engineering*, 57(4), 337–345.
- Tamura, Y., Tsurumi, N., & Matsumoto, Y. (2014). Visualizations of bubble motions and temperature rises by focused ultrasound. *Procedia Engineering*, 90, 5–10.
- Wang, L. J., & Sun, D.-W. (2001). Rapid cooling of porous and moisture foods by using vacuum cooling technology. *Trends in Food Science & Technology*, 12, 174–184.
- Xie, A., Sun, D.-W., Xu, Z., & Zhu, Z. (2015). Rapid detection of frozen pork quality without thawing by Vis-NIR hyperspectral imaging technique. *Talanta*, 139, 208–215.
- Xie, A., Sun, D.-W., Zhu, Z., & Pu, H. (2016). Nondestructive measurements of freezing parameters of frozen porcine meat by NIR hyperspectral imaging. *Food and Bioprocess Technology*, 9, 1444–1454.
- Xin, Y., Zhang, M., & Adhikari, B. (2014). Ultrasound assisted immersion freezing of broccoli (*Brassica oleracea* L. var. *botrytis* L.). *Ultrasonics Sonochemistry*, 21(5), 1728–1735.
- Xu, B., Zhang, M., Bhandari, B., Cheng, X., & Sun, J. (2015). Effect of ultrasound immersion freezing on the quality attributes and water distributions of wrapped red radish. *Food and Bioprocess Technology*, 8(6), 1366–1376.
- Yang, Q., Sun, D.-W., & Cheng, W. (2017). Development of simplified models for nondestructive hyperspectral imaging monitoring of TVB-N contents in cured meat during drying process. *Journal of Food Engineering*, 192, 53–60.
- Zheng, L., & Sun, D.-W. (2006). Innovative applications of power ultrasound during food freezing processes : a review. *Trends in Food Science and Technology*, 17(1), 16–23.